

Predicting Solute Transport Parameters in Saturated Porous Media Using Hybrid Algorithm

Bouredji, Hamza*⁺; Bendjaballah Lalaoui, Nadia; Rennane, Samira

Laboratoire de Matériaux Catalytiques et Catalyse en Chimie Organique, Université des Sciences et de la Technologie Houari Boumediène, Alger, ALGÉRIE

Merzougui, Abdelkrim

Laboratoire de Recherche en Génie Civil, Hydraulique, Développement Durable et Environnement, Université Mohamed Kheider, Biskra, ALGÉRIE

ABSTRACT: This study aims to estimate the solute transport parameters in saturated porous media using a hybrid algorithm. In this study, the Physical Non-Equilibrium (PNE) model was used to describe the transport of solutes in porous media. A numerical solution for the PNE model is obtained using the Finite Volume Method (FVM) based on the Tri-Diagonal Matrix Algorithm (TDMA). The developed program, written in Matlab, is capable to solve the advection-dispersion (ADE) and the PNE equations for the mobile-immobile (MIM) model with linear sorption isotherm. The Solute transport parameters, (immobile water content, mass transfer coefficient, and dispersion coefficient), are estimated using different algorithms such as the Levenberg-Marquardt algorithm (LM), genetic algorithm (GA), simulated annealing algorithm (SA). To overcome the limitations of deterministic optimization models which are rather unstable and divergent around a local minimum, a hybrid algorithm (GA+LM, SA+LM) permits to estimate of the solute transport parameters. Numerical solutions are verified using the experiments conducted by Semra (2003) which are about the transport of toluene through a column composed of impregnated Chromosorb grains at ambient temperature (20 °C) for three flow rates (1, 2 and 5ml/min). The results show that the hybrid algorithm (GA+LM, SA+LM) is more accurate than others (GA, SA, and LM). Comparing to the ADE model, The PNE with linear isotherm model gives a better description to the Breakthrough Curves (BTCs) with higher values of determination coefficient (R^2) and lower values of Root Mean Square Error (RMSE). Also, the solute transport parameters tended to vary with the flow rate.

KEYWORDS: Genetic algorithm; Finite volume method; Levenberg-Marquardt algorithm; Numerical solution; Physical non-equilibrium.

INTRODUCTION

Prediction of the transport of solute in porous media is important to evaluate contamination in soils and aquifers. The advection-dispersion equation (ADE) is often used

to describe the solute transport in soils undersaturated and unsaturated conditions. Dispersion coefficient, one of the parameters of ADE, is a measure of dispersive properties

*To whom correspondence should be addressed.

+E-mail: bouredjih@gmail.com

1021-9986/2020/6/945-954

10/\$/6.00

of soil. In the literature, several models are proposed for prediction of dispersion coefficient. In one dimension, the dispersion coefficient is defined mathematically as a linear function of the water velocity and a constant which corresponds to the longitudinal dispersivity [30]. At column scale, dispersivity between 0.01 and 1.0 cm *Zheng and Bennett* [30], *Perkins and Johnston* [19] found an empirical relation to calculate the dispersivity according to the particle diameter. Another empirical relation is also given by *Zheng and Bennett* [30] to calculate the dispersivity according to the length of the column.

The physical non equilibrium (PNE) model is often used to calibrate the experimental results by optimization of model parameters. The model divides the pore space into “mobile” and “immobile” flow regions with first-order mass transfer between these two regions.

Application of the PNE model requires the estimation of three parameters. (θ_{im}), the immobile water content, (α), the mass transfer coefficient between mobile and immobile water region, and the dispersion coefficient in mobile water or (D_m). For most applications, these three parameters are difficult to estimate. It is suitable to obtain such parameters based on experimental methodologies. Consequently, these parameters must be optimized using inverse methods to the solute concentrations in the column outflow vs. time [21]. Inverse methods applied to solute breakthrough curves are typically used to estimate the parameter values [28].

A common way of estimating the mobile and immobile water content is to use the curve fitting of tracer breakthrough results [22], based on the following mass balance equation:

$$\theta C = \theta_m C_m + \theta_{im} C_{im} \quad (1)$$

When α is small enough to assume the concentration in immobile water (C_{im}) negligible and C_0 is the input concentration at certain infiltration time t , an approximate equation is obtained $\theta_{im} = \theta (1 - C/C_0)$. Applications of this method can be found in *Clothier et al.* [3], and *Jaynes et al.* [8]. Assuming that the concentration in the mobile water (C_m) equals the input concentration C_0 , *Jaynes et al.* [8] used the following formula:

$$\ln(1-C/C_0) = at + b \quad (2)$$

Where $a = -\alpha / \theta_{im}$ and $b = \ln(\theta_{im} / \theta)$.

θ_m and θ_{im} can be evaluated by plotting $\ln(1-C/C_0)$ versus elapsed time. However, the assumption of $C_m = C_0$ associated with this method is debatable and may not be correct as long as $\alpha > 0$, Slightly different from the approach of *Jaynes et al.* [8] and *Clothier et al.* [3], *Goltz and Roberts* [7] estimated the fraction of mobile water as the ratio of velocity calculated from hydraulic conductivity to the velocity measured from tracer experiment. Several examples are available on various parameters estimation associated with the mobile immobile approach. For unsaturated glass beads with diameters in the neighborhood of 100 μm , *De Smedt and Wierenga* [5] found $\theta_m = 0.853 \theta$. For dispersion coefficient in mobile water, three models for dispersion coefficient were presented by *Sharma et al.* [25], the Mobile-Immobile model for constant dispersion (MIMC), linear distance dependent dispersion (MIML), and exponential distance dependent dispersion (MIME). The comparison of these models shows that the MIM model with constant and exponential distance-dependent dispersion can be used for simulation of the breakthrough curves.

To date, different global optimization techniques have been reported for the solute transport modeling, including a variety of stochastic global optimization methods [17]. As example, the genetic algorithm (GA), simulated annealing (SA), tabu search (TS), bees algorithm (BA) and successive equimarginal approach (SEA) have been reported as promising optimization methods [12, 17] and can be used for solute transport calculations. In particular, *Giacobbo et al.* [6] studied the transport of contaminants through a three-layered monodimensional saturated medium by a numerical solution of advection dispersion equation and apply GA to evaluate the hydrodynamic dispersion coefficient and the fluid velocity. Their results indicate that the method is capable to estimate the parameters values with accuracy.

It is convenient to remark that the stochastic global optimization methods show disadvantages depending on the optimization problem under analysis, which could include a low convergence performance especially for multivariable problems.

In the present paper, we propose a combination of a stochastic global optimization method GA or SA with Levenberg-Marquardt algorithm (LM), used to improve the results of GA or SA methods. The motivation of using

such a method is to avoid stopping on a local minimum obtained by the GA or SA methods.

THEORETICAL

Problem formulation

The transport of a solute in a porous medium (soil) with mobile and immobile regions of soil water is governed by the following equations [10]:

$$\rho \frac{\delta S_m}{\delta t} + \rho \frac{\delta S_{im}}{\delta t} + \Theta_m \frac{\delta C_m}{\delta t} + \Theta_{im} \frac{\delta C_{im}}{\delta t} = \tag{3}$$

$$-u_m \Theta_m \frac{\delta C_m}{\delta x} + D_m \Theta_m \frac{\partial^2 C_m}{\partial x^2} + \Theta_{im} \frac{\delta C_{im}}{\delta t} + \rho \frac{\delta S_{im}}{\delta t} = \alpha (C_m - C_{im}) \tag{4}$$

Where u_m is the pore-water velocity in the mobile water [L/T], C_m, C_{im} the solute concentration in the mobile and immobile water respectively [M/L³], S_m, S_{im} the solid phase concentration of solute from either the mobile and immobile region per mass of dry soil respectively [M/M], D_m the dispersion coefficient in the mobile water [L²/T], ρ the dry soil bulk density [M/L³], α the mass transfer coefficient between mobile and immobile region [1/T], Θ_m and Θ_{im} the mobile and immobile water contents [L³/L³], x the direction, and t the time [T].

The linear sorption isotherm assumes that the sorbed concentrations S_m, S_{im} for mobile and immobile regions are directly proportional to the dissolved concentration C_m, C_{im} :

$$S_m = K_d C_m \tag{5a}$$

$$S_{im} = K_d C_{im} \tag{5b}$$

With K_d a “distribution” constant expressed as volume of aqueous phase per mass of dry soil [L³/M].

In such a case, the equation (3) can be written as:

$$\left(1 + \frac{\rho K_d}{\Theta_m} \right) \frac{\delta C_m}{\delta t} + \left(\frac{\Theta_{im}}{\Theta_m} + \frac{\rho K_d}{\Theta_m} \right) \frac{\delta C_{im}}{\delta t} = \tag{6}$$

$$D_m \frac{\partial^2 C_m}{\partial x^2} - u_m \frac{\delta C_m}{\delta x}$$

This equation describes the physical non equilibrium equation combined with linear isotherm model. Notice that if $\Theta_{im}=0$, equation (6) is reduced to ADE with linear

isotherm model (equation 7).

$$\left(1 + \frac{\rho K_d}{\Theta} \right) \frac{\delta C}{\delta t} = D_m \frac{\partial^2 C}{\partial x^2} - u_m \frac{\delta C}{\delta x} \tag{7}$$

Numerical solution

Using dimensionless variables, the two transport Equations (3), (4) become:

$$\int_0^L \frac{\delta C_m^*}{\delta x^*} dx \Big|^{t+\Delta t} + \int_0^L R_m \frac{d_p}{L} \frac{\delta C_m^*}{\delta t^*} dx \Big|^{t+\Delta t} + \tag{8}$$

$$\int_0^L \frac{\Theta_{im}}{\Theta_m} R_{im} \frac{d_p}{L} \frac{\delta C_{im}^*}{\delta t^*} dx \Big|^{t+\Delta t} = \int_0^L \frac{1}{P_e} \frac{\partial^2 C_m^*}{\partial x^{*2}} dx \Big|^{t+\Delta t}$$

$$\int_0^L \Theta_{im} R_{im} \frac{\delta C_{im}^*}{\delta t^*} dx \Big|^{t+\Delta t} = \int_0^L \frac{L\alpha}{u_m} (C_m^* - C_{im}^*) dx \Big|^{t+\Delta t} \tag{9}$$

Where: $R_m = 1 + \rho K_d / \Theta_m$, $R_{im} = 1 + \rho K_d / \Theta_{im}$,

$$t^* = \frac{u_m}{L} t, C^* = \frac{C}{C_0}, x^* = \frac{x}{d_p}, P_e = \frac{d_p u_m}{D_m}$$

C_0 is the input concentration [M/L³], d_p the diameter of soil particle [L] and L the column length [L].

The dimensionless equation (9) has been solved using the finite volume method according to second order Euler backward (Fig .1) and the Adam Bashforth scheme [17].

After simplification, we can establish the following relationship:

$$C_{im(i)}^{*t+\Delta t} = \frac{2\Delta t L \alpha}{3\Theta_{im} R_{im} + \frac{2\Delta t L \alpha}{u_m}} (C_{m(i)}^*)^{t+\Delta t} - \tag{10}$$

$$\frac{\Theta_{im} R_{im}}{3\Theta_{im} R_{im} + \frac{2\Delta t L \alpha}{u_m}} (-4C_{im(i)}^{*t} + C_{im(i)}^{*t-\Delta t})$$

Equation (10) gives the dimensionless immobile concentration at time $(t+\Delta t)$ according to dimensionless mobile concentration at time $(t+\Delta t)$.

We use the same method to solve the dimensionless Equation (8), we substitute the Equation (10) into the solved equation to obtain the following expression:

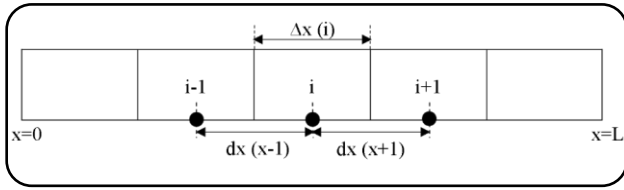


Fig. 1: Numerical grid for the one dimensional column laboratory.

$$A_{(i)} \left(C_{m(i)}^* \right)^{t+\Delta t} = A_{(i+1)} \left(C_{m(i+1)}^* \right)^{t+\Delta t} + \quad (11)$$

$$A_{(i-1)} \left(C_{m(i-1)}^* \right)^{t+\Delta t} + Sr$$

Where:

$$A_{(i)} = \frac{3d_p \Delta x(i)}{2L\Delta t} R_m + \frac{1}{P_e} \left(\frac{1}{dX(i+1)} + \frac{1}{dX(i-1)} \right) + \quad (12a)$$

$$\frac{3d_p \alpha \Delta x(i)}{\Theta_m u_m} \frac{\Theta_{im} R_{im}}{3\Theta_{im} R_{im} + \frac{2\alpha L \Delta t}{u_m}}$$

$$A_{(i+1)} = \frac{1}{P_e dX(i+1)} \quad (12b)$$

$$A_{(i-1)} = \frac{1}{P_e dX(i-1)} \quad (12c)$$

$$Sr = - \left[\left(C_{m(i+1)}^* \right)^t - \left(C_{m(i-1)}^* \right)^t - \quad (12d)$$

$$\frac{\left(C_{m(i+1)}^* \right)^{t-\Delta t} - \left(C_{m(i-1)}^* \right)^{t-\Delta t}}{2} \right] - \frac{d_p \Delta x(i)}{2L\Delta t} R_m \left(-4C_{m(i)}^{*t} + C_{m(i)}^{*t-\Delta t} \right)$$

$$- \frac{d_p \Delta x(i)}{2L \cdot \Delta t} \frac{\Theta_{im} R_{im}}{\Theta_m} \left[- \frac{3\Theta_{im} R_{im}}{3\Theta_{im} R_{im} + \frac{2\Delta t L \alpha}{u_m}} + 1 \right] \left(-4C_{m(i)}^{*t} + C_{m(i)}^{*t-\Delta t} \right)$$

Equation (11) is a system of equations which form tri-diagonal matrix that can be solved by the Thomas algorithm [17].

The initial and boundary conditions (Dirichlet) are:

$$C_m(x, 0) = 0, \quad C_m(0, t) = C_0, \quad \left(\frac{\partial C_m}{\partial x} \right)_{x=L} = 0$$

Solute transport parameters estimation

The different solute transport parameters are obtained from experimental data by minimizing a suitable objective function. The most common objective function is the sum

of the square of the error between the experimental and calculated relative concentrations, the objective function can be defined as [9]:

$$\min F = \sum_{i=1}^n \left(C_i^m - C_i^e \right)^2 \quad (13)$$

Where C_i^m is the measured relative concentration and C_i^e the estimated relative concentration.

Both the determination coefficient (R^2) and the root mean square error (RMSE) were used as two criteria to reflect the goodness of simulation [24]:

$$R^2 = 1 - \frac{\sum_{i=1}^n \left(C_i^m - C_i^e \right)^2}{\sum_{i=1}^n \left(C_i^m - \overline{C_i^m} \right)^2} \quad (14)$$

$$RMSE = \sqrt{\frac{1}{n} \sum_{i=1}^n \left(C_i^m - C_i^e \right)^2} \quad (15)$$

Where $\overline{C_i^m}$ represent the mean values of C_i^m , and n the number of measurements.

To determine the solute transport parameters, the levenberg-marquardt algorithm (LM), genetic algorithm (GA) and simulated annealing algorithm (SA) were used that are presented by the MATLAB functions "lsqcurvefit", "ga" and "simulannealbnd", respectively. The parameters used by MATLAB for GA and SA algorithm are given in Table 1.

In order to improve the fitting of the breakthrough curves, the non-classical algorithms (GA, SA) and classical method of Levenberg–Marquardt were hybridized. The basic step of the algorithm is to use the obtained values of solute transport parameters by GA or SA as start point to be used by Levenberg–Marquardt; then we calculate new values of solute transport parameters by the Levenberg–Marquardt method.

For all algorithms, before optimization of parameters, we specified the lower and upper bounds also the start point given in literature:

$$D_m(m^2/s) \in [10^{-14}, 0.1], \quad \theta_{im} \in [10^{-14}, 0.1] \text{ and } \alpha (s^{-1}) \in [10^{-14}, 0.1]$$

$$\text{Start point: } D_m = 0.1 \text{ m}^2/\text{s}, \quad \theta_{im} = 0.1, \quad \alpha = 0.1 \text{ s}^{-1}.$$

The solute transport parameters of PNE model are unknown. They are determined by an inverse method by comparing experimental results with those of the simulation. It is the whole purpose of this work after

Table 1: Parameters setting of the GA and SA algorithm.

Algorithms	GA	SA
Parameters setting	Population type: Double vector	Annealing function: Fast annealing
	Population size: 50	Initial temperature: 100
	No. of generation: 100	Tolerance: 10^{-6}
	Selection strategy: Roulette	Update function T: Exponential T update
	Crossover type: One point	
	Crossover probability: 0.80	
	Mutation probability: 0.01	
	Tolerance: 10^{-6}	

solving the Equation (11) by using the finite volume method, the hybrid algorithm is used to minimize the objective function of Eq. (13). The hybrid algorithm calculates in a final way the unknown three parameters (see Fig. 2).

EXPERIMENTAL DATA

To validate the models developed in our study, we used the experimental data of *Semra* [23] that used an experimental protocol for front-end chromatography. It consists of HPLC pump, a glass column with adjustable bed height thanks to two pistons, a short-circuit at the ends of the column, a conductivity meter and an in-line U.V detector. The body of the pump (pistons and sintered) is made of stainless steel to avoid the adsorption of the organic tracers. The pipes and valves are Teflon but their low exchange surface makes it possible to neglect the adsorption phenomenon (see Fig. 3).

The toluene adsorption isotherm by Chromosorb (Copolymer of styrene and divinylbenzene) impregnated with oil HMN (Hyptaméthylnonane) was determined at ambient temperature (20 °C) on a column composed of impregnated Chromosorb grains, non-reactive with toluene. These experiments are realized for three flow rates (1, 2 and 5 ml/min). Table 2 summarizes the experimental data of the column and porous medium.

RESULTS AND DISCUSSION

Table 3 presents the different optimization algorithms used to evaluate the solute transport parameters which are LM, GA, SA and their hybrid algorithm namely (GA+LM, SA+LM) for the two models ADE and PNE. As shown in Table 3, the hybrid algorithm gives better results for the

PNE model. We note that all algorithms used in the optimization give approximately the same values of dispersion coefficient for ADE model. Consequently, the same fitting of breakthrough curves. Comparing to the ADE model, the PNE model gives a better description of breakthrough curves with higher value of R^2 and lower value of RMSE (Fig. 4).

The results obtained by the PNE model using the hybrid algorithm show that the dispersion coefficient increases with raising the flow rate, with: 3.49×10^{-7} , 8.23×10^{-7} and $3.76 \times 10^{-6} \text{ m}^2/\text{s}$ for 1, 2 and 5 ml/min respectively. Similar results were obtained by *Suresh et al.* [26].

The values obtained of immobile water content and mass transfer coefficient are compared with the literature, *Masciopinto and Passarella* [12] estimate the coefficient of the mass transfer during the step injection of NaCl. The α -values ($\sim 10^{-5} \text{ s}^{-1}$) are close to those of *Padilla et al.* [16] which studied the transport of NaCl through saturated porous media, their obtained value of immobile water content equal to 10^{-2} which is roughly equal to our results (Table 3).

The immobile water content changes with the flow rate, which decreases from 1.03×10^{-1} to 6.89×10^{-2} for 1 to 2 mL/min furthermore it increases to 9.90×10^{-2} for 5 mL/min. These results indicate when the immobile water content decreases the solute must travel longer distances or times between mobile and immobile regions, and vice versa. This variation of the flow rate influences on the mass transfer coefficient, this latter augments from 3.84×10^{-5} to $2.06 \times 10^{-4} \text{ s}^{-1}$ for 1 to 2 ml/min furthermore it reduces to $8.38 \times 10^{-6} \text{ s}^{-1}$ for 5 ml/min. This variation of the mass transfer coefficient is due to the variation of immobile water content which is related with transfer resistance. The increase of the mass transfer coefficient

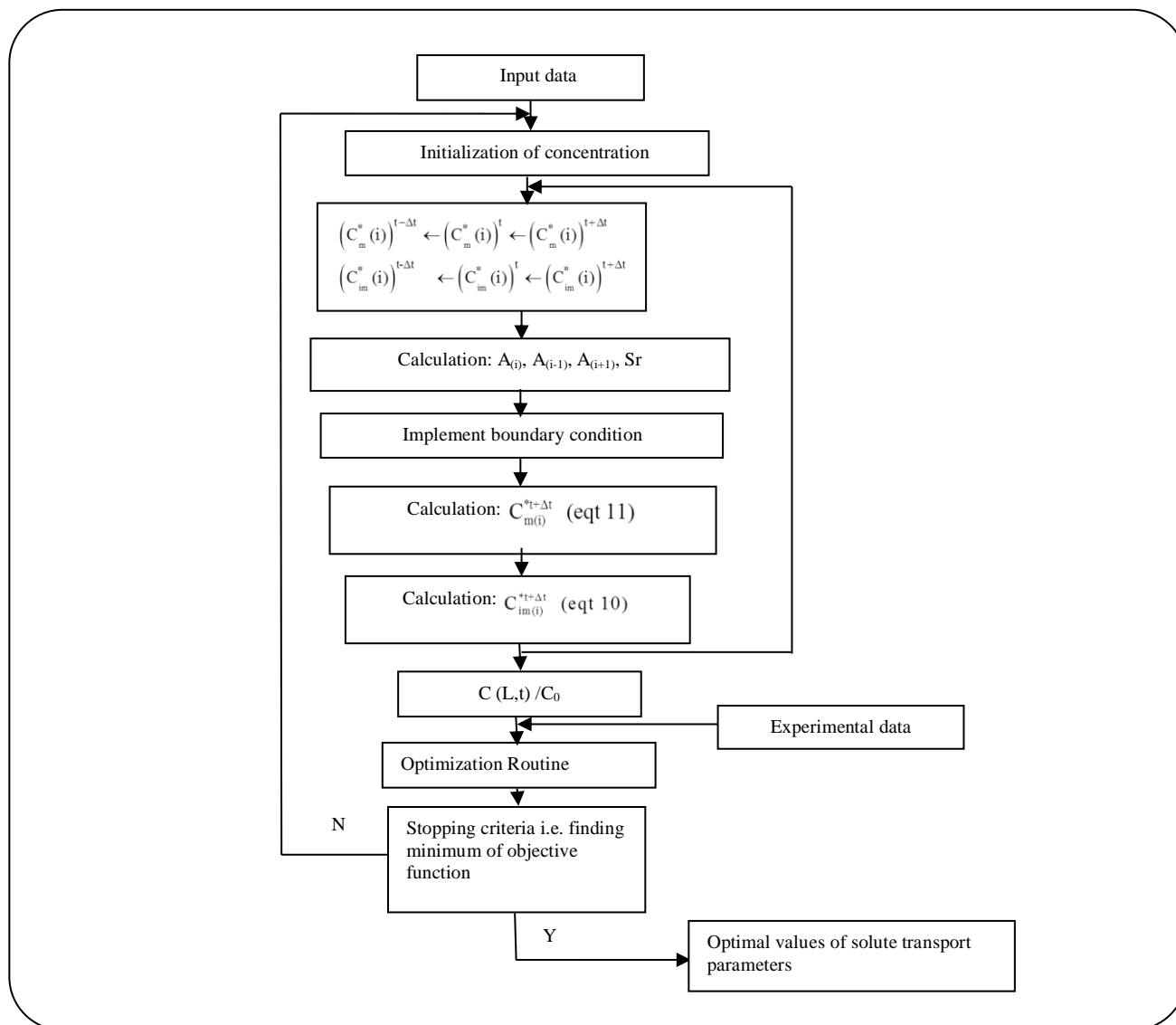


Fig. 2: The flowchart for evaluating solute transport parameters.

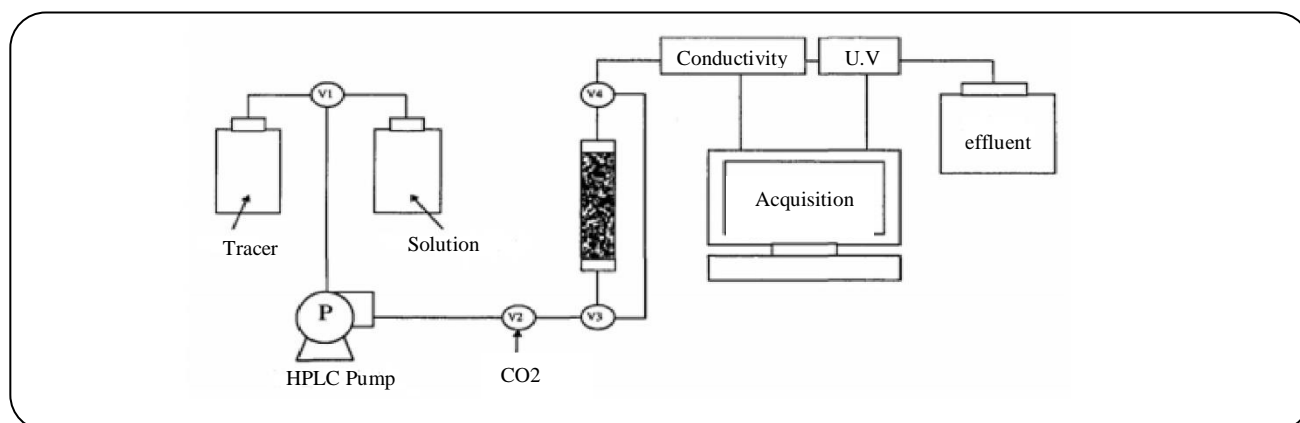


Fig. 3: The experimental editing used by Semra [23].

Table 2: Experimental data of column and porous medium (Semra, 2003).

Column diameter(cm)	L (cm)	K_d (l/kg HMN)	ρ (g/cm ³)	d_p (μ m)	Θ (cm ³ /cm ³)
1	6.4	671	0.505	215	0.836

Table 3: Optimization of solute parameters.

Flow rate (mL/min)	Models	Tools	D_m (m ² /s) $\times 10^7$	Θ_{im}	α (s ⁻¹) $\times 10^5$	Fobj $\times 10^3$	R ²	RMSE
1	PNE	LM	3.98	0.199	3.34	7.70	0.9978	0.0169
		GA	3.80	0.0998	3.90	8.30	0.9977	0.0176
		SA	3.40	0.0966	7.69	8.10	0.9977	0.0173
		GA+LM	3.49	0.103	3.84	6.60	0.9982	0.0156
		SA+LM	3.51	0.107	3.91	6.70	0.9981	0.0158
	ADE	LM	3.11	-	-	7.50	0.9979	0.0167
		GA	3.17	-	-	7.60	0.9979	0.0168
		SA	3.09	-	-	7.60	0.9979	0.0167
2	PNE	LM	10.5	0.250	23.2	14.7	0.9961	0.0233
		GA	8.77	0.0995	21.4	15.2	0.9966	0.0218
		SA	8.20	0.0680	21.5	14.8	0.9967	0.0215
		GA+LM	8.55	0.0995	21.3	15.0	0.9966	0.0217
		SA+LM	8.23	0.0689	20.6	14.7	0.9967	0.0214
	ADE	LM/GA/SA	7.74	-	-	25.9	0.9942	0.0284
5	PNE	LM	37.4	0.0957	2.85	0.156	0.9999	0.0026
		GA	37.7	0.0993	0.553	0.140	0.9999	0.0025
		SA	47.9	0.267	8.30	0.224	0.9999	0.0031
		GA+LM	37.6	0.0990	0.838	0.137	0.9999	0.0024
		SA+LM	35.5	0.0517	1.66	0.157	0.9999	0.0026
	ADE	LM/GA/SA	33.3	-	-	0.150	0.9999	0.0026

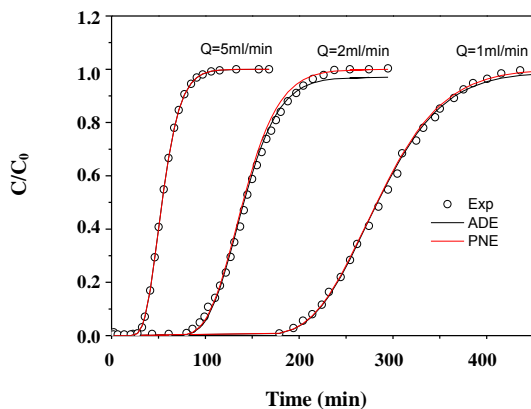


Fig. 4: Comparison of concentration calculated with PNE and ADE models and the experimental data.

is referred to higher mixing in the mobile phase at high flow rate [21] or to shorter diffusion path lengths as a result of a decrease in the amount of immobile water [28]. To clarify this study, other experimental data must be realized at supplementary flow rates to obtain a correlation between the mass transfer coefficient, the immobile water content and the flow rate.

The experimental and the best predicted concentrations using different optimization algorithms for ADE and PNE models are given in Fig.5. Residuals (e_i) plots for measured concentration are also reported in Fig.6.

The coefficients R^2 for the regression of observed versus fitted concentrations show that the PNE yields a better overall fit ($0.9967 < R^2 < 0.9999$) than the ADE model ($0.9942 < R^2 < 0.9999$). The plots of measured

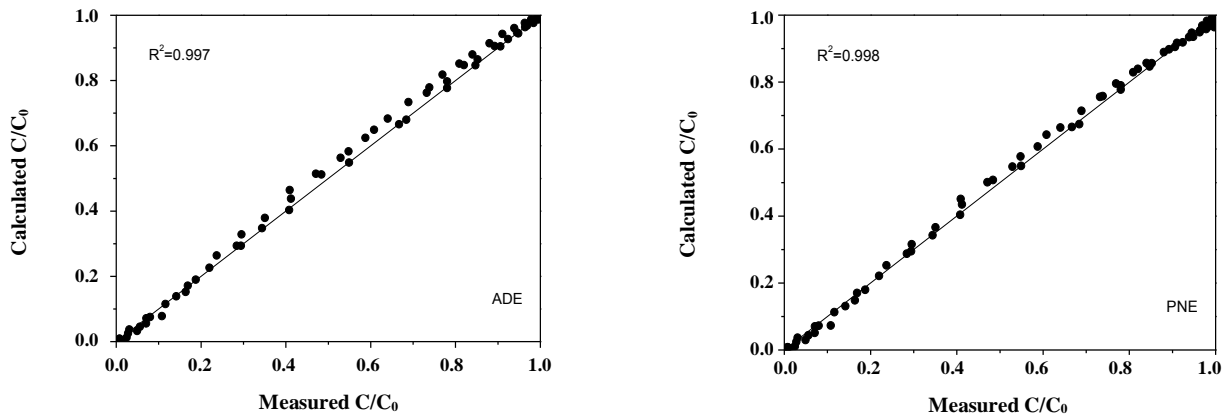


Fig. 5: Fitting measured and calculated concentration with PNE and ADE models.

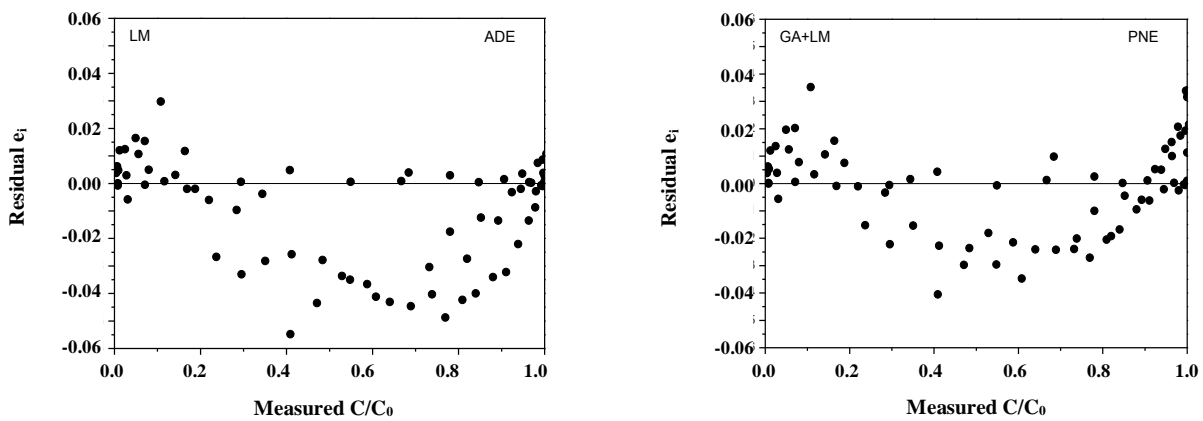


Fig. 6: Residual plots of calculated concentration modeled with PNE and ADE.

versus simulated relative concentrations show that PNE-simulated C/C_0 fall on a 45° line, whereas those of the ADE model are scattered about this line (Fig. 5). This suggests that the relative concentrations (C/C_0) measured are better represented by the PNE simulated C/C_0 values than those from the ADE model.

In general, residual plots of PNE and ADE showed a random distribution but with different error variances. This residual analysis also confirms that the hybrid algorithm was the best option for solute transport data fitting. Objective functions values decreased from 7.5×10^{-3} to 6.6×10^{-3} for flow rate 1 ml/min, from 2.59×10^{-2} to 1.47×10^{-2} for flow rate 2 ml/min and from 1.5×10^{-4} to 1.37×10^{-4} for flow rate 5 ml/min (Table 3).

In addition, Fig. 6 shows the mean modeling errors for the prediction of concentrations. These modeling errors

ranged from 3.1 to 5.6 % for LM and from 3.6 to 4.1 % for GA+LM. The modeling performance of GA+LM was better than those obtained with LM.

Finally, the application of hybrid algorithms on PNE model can be used to handle the experimental data of the solute transport in saturated porous media.

CONCLUSIONS

In this study, we have presented a one-dimensional model that describes the transport of contaminants in a column laboratory. A numerical algorithm has been presented to solve PNE and ADE models. A semi-stochastic method proposed to estimate the solute transport parameters which is a combination of stochastic method (GA, SA) with deterministic optimization models (LM). The performance of GA, SA and LM algorithms have been

tested and compared with hybrid algorithms (GA+LM), (SA+LM) for the solute transport modeling using experimental data. In most cases, the average root mean square error obtained by hybrid algorithms (GA+LM), (SA+LM) is relatively better than the other ones algorithms. A better description of breakthrough curves was providing by the PNE combined with linear isotherm model; it is found that the PNE parameter values (immobile water content, mass transfer coefficient and dispersion coefficient) tend to vary with the flow rate.

Received :Sept, 2019 ; Accepted : Jan. 13, 2020

REFERENCES

- [1] Alwan G.M., [Improving Operability of Lab-Scale Spouted Bed Using GlobalStochastic Optimization](#), *Journal of Engineering Research and Applications*,**5**: 136-146 (2015).
- [2] Chen Y.M., Abriola L.M., Alvarez P.J.J., Anid P.J., Vogel T.M., [Modeling Transport and Biodegradation of Benzene and Toluene in Sand Aquifer Material: Comparison with Experimental Measurements](#), *Water Resour. Res.*, **28**(7): 1833-1847 (1992).
- [3] Clothier B.E., Kirkham M.B., Mclean J.E., [In Situ Measurement of the Effective Transport Volume for Solute Moving Through Soil](#), *Soil Sci. Soc. Am. J.*,**56**: 733-736 (1992).
- [4] Coats K.H., Smith B.D., [Dead-End Pore Volume and Dispersion in Porous Media](#). *Soc. Pet. Eng. J.*, **4**: 73-84 (1964).
- [5] De Smedt F., Wierenga P.J., [Solute Transfer Through Columns of Glass Beads](#), *WaterResour. Res.*, **20**: 225-232 (1984).
- [6] Giacobbo F., Marseguerra M., Zio E., [Solving the Inverse Problem of Parameter Estimation by Genetic Algorithms: The Case of a Groundwater Contaminant Transport Model](#), *Annals of Nuclear Energy*,**29**: 967-981 (2002).
- [7] Goltz M.N., Roberts P.V., [Simulations of Physical Nonequilibrium Solute Transport Models: Application to a Large Scale Field Experiment](#), *J. Contamin. Hydrol.*, **3**:37-63(1988).
- [8] Jaynes D.B., Logsdon S.D., Horton R., [Field Method for Measuring Mobile/Immobile Water Content and Solute Transfer Rate Coefficient](#), *Soil Sci. Soc. Am. J.*, **59**: 352-356 (1995).
- [9] Kabouche A., Meniai A., Hasseine A., [Estimation of Coalescence Parameters in an Agitated Extraction Column Using a Hybrid Algorithm](#), *Chem. Eng. Technol.*,**34**(5): 784-790 (2011).
- [10] Leij F.J., Bradford S.A., [Combined Physical and Chemical Nonequilibrium Transport Model: Analytical Solution, Moments, and Application to Colloids](#), *J. Contam. Hydrol.*,**110**: 87-99 (2009).
- [11] Manuel Alejandro Salaices Avila, ["Experiment and Modeling of the Competitive Sorption And Transport of Chlorinated Ethenes in Porous Media"](#), Göttingen-Germany, (2005).
- [12] Masciopinto C., Passarella G., [Mass-Transfer Impact on Solute Mobility in Porous Media: a New Mobile-Immobile Model](#), *J. Contam. Hydrol.*,**215**: 21-28 (2018).
- [13] Mehdinejadi B., [Estimating the Solute Transport Parameters of the Spatial FractionalAdvection-Dispersion Equation Using Bees Algorithm](#), *J. Contam. Hydrol.***203**: 51-61 (2017).
- [14] Merzougui A., Hasseine A., Laiadi D., [Liquid-Liquid Equilibria of {N-Heptane + Toluene + Aniline} Ternary System: Experimental Data and Correlation](#), *Fluid Phase Equilib.* **308**: 142-146 (2011).
- [15] Nelson P.A., Galloway, T.R., [Particle to Fluid Heat and Mass Transfer in Dense System to Fine Particles](#), *Chemical Engineering Science.* **30**: 1-6 (1975).
- [16] Padilla I.Y., Jim Yeh T.-C., Conklin M.H., [The Effect of Water Content on Solute Transport in Unsaturated Porous Media](#), *Water Resources Research*, **35**: 3303-3313 (1999).
- [17] Patankar S.V., ["Numerical Heat Transfer And Fluid Flow"](#), USA: New York, Mcgraw-Hill Book Company, (1980).
- [18] Peralta R.C., ["Groundwater Optimization Handbook: Flow, Contaminant Transport, and Conjunctive Management"](#), Boca Raton, CRC Press, p.532, (2012).
- [19] Perkins T.K., Johnston O.C., [A Review of Diffusion and Dispersion in Porous Media](#), *Society of Petroleum Engineers Journal*,**3**: 7&84, (1963).
- [20] Sardin M., Schweich D., Leij F.J., Van Genuchten M.Th., [Modeling the Nonequilibrium Transport of Linearly Interacting Solutes in Porous Media: a Review](#), *Water Resources Research*,**27**: 2287-2307 (1991).

- [21] Selim H.M., Ma L., "Physical Non-Equilibrium in Soils: Modeling and Application", Ann Arbor Press, Inc., Chelsea, Mich, (1998).
- [22] Selim H.M., "Transport & Fate of Chemicals in Soils Principles & Applications", CRC Press, (2015).
- [23] Semra S., "Dispersion Réactive En Milieu Poreux Naturel", Thèse, Génie Des Procédés. Nancy, INPL, (2003).
- [24] Shahram Shahmohammadi-Kalalagh, Modeling Contaminant Transport In Saturated Soil Column With The Continuous Time Random Walk, *Journal Of Porous Media*, **18**: 1181-1186 (2015).
- [25] Sharma P.K., Shukla S.K., Rahul Choudhary, Deepak Swami, Modeling for Solute Transport in Mobile-Immobile Soil Column Experiment, *ISH Journal of Hydraulic Engineering*, (2016).
- [26] Suresh A.Kartha, Srivastava R., Effect of Immobile Water Content Contaminant Transport in Unsaturated Zone, *Journal of Hydro-Environment Research*, **1**: 206-215 (2008).
- [27] Van Genuchten M.Th., Cleary R.W., "Movement of Solutes in Soil: Computer Simulated And Laboratory Results", Chap. 10 In: Soil Chemistry: B. Physicochemical Model, G.H. Bolt, (Ed.), Elsevier, Amsterdam, (1979).
- [28] Van Genuchten M. Th., Non-Equilibrium Transport Parameters From Miscible Displacement Experiments, Res. Rep. No. 119, U.S. Salinity Lab. USDA, ARS, Riverside, CA, (1981).
- [29] Van Viet Ngo, "Modélisation Du Transport De L'eau Et Des Hydrocarbures Aromatiques Polycycliques (HAP) Dans Les Sols De Friches Industrielles", Thèse De Doctorat INPL, Nancy-France, 172 P, (2009).
- [30] Zheng C., Bennet G.D., "Applied Contaminant Transport Modeling: Theory and Practice", van Nostrand Reinhold, New York, 464 P, (1995).